

Schottky-contacted vertically self-aligned ZnO nanorods for hydrogen gas nanosensor applications

Sapana Ranwa, Mohit Kumar, Jitendra Singh, Mattia Fanetti, and Mahesh Kumar

Citation: [Journal of Applied Physics](#) **118**, 034509 (2015); doi: 10.1063/1.4926953

View online: <http://dx.doi.org/10.1063/1.4926953>

View Table of Contents: <http://scitation.aip.org/content/aip/journal/jap/118/3?ver=pdfcov>

Published by the [AIP Publishing](#)

Articles you may be interested in

[Si/ZnO nanorods/Ag/AZO structures as promising photovoltaic plasmonic cells](#)

J. Appl. Phys. **117**, 193101 (2015); 10.1063/1.4921424

[Defect-free ZnO nanorods for low temperature hydrogen sensor applications](#)

Appl. Phys. Lett. **105**, 213103 (2014); 10.1063/1.4902520

[Effect of Sn doping on morphology and ethanol sensing response of ZnO nanorods](#)

AIP Conf. Proc. **1447**, 429 (2012); 10.1063/1.4710063

[Gold coated ZnO nanorod biosensor for glucose detection](#)

AIP Conf. Proc. **1447**, 295 (2012); 10.1063/1.4709996

[Role of near-surface states in ohmic-Schottky conversion of Au contacts to ZnO](#)

Appl. Phys. Lett. **87**, 012102 (2005); 10.1063/1.1984089

An advertisement for the journal AIP APL Photonics. The background is a vibrant orange and red gradient with a bright sunburst effect on the right. On the left, there is a small image of the journal cover, which features a blue and white abstract design. A yellow starburst graphic with the words 'OPEN ACCESS' is overlaid on the bottom right of the journal cover. To the right of the journal cover, the text 'Launching in 2016!' is written in a large, white, sans-serif font. Below this, the text 'The future of applied photonics research is here' is written in a smaller, white, sans-serif font. At the bottom right, the AIP APL Photonics logo is displayed in white.

Schottky-contacted vertically self-aligned ZnO nanorods for hydrogen gas nanosensor applications

Sapana Ranwa,¹ Mohit Kumar,¹ Jitendra Singh,² Mattia Fanetti,³ and Mahesh Kumar^{1,a)}

¹Department of Electrical Engineering, Indian Institute of Technology Jodhpur, Jodhpur 342011, India

²Sensors and Nanotechnology Group, CSIR-Central Electronics Engineering Research Institute, Pilani, Rajasthan 333031, India

³Materials Research Laboratory, University of Nova Gorica, Vipavska 11c, SI-5270 Ajdovščina, Slovenia

(Received 4 June 2015; accepted 4 July 2015; published online 20 July 2015)

Vertically well aligned ZnO nanorods (NRs) were grown on Si(100) substrate using RF magnetron sputtering technique. Scanning electron microscopy images confirms uniform distribution of NRs on 2 in. wafer with average diameter, height and density being ~ 75 nm, ~ 850 nm, and $\sim 1.5 \times 10^{10} \text{ cm}^{-2}$, respectively. X-ray diffraction reveals that the ZnO NRs are grown along c-axis direction with wurtzite crystal structure. Cathodoluminescence spectroscopy, which shows a single strong peak around 3.24 eV with full width half maxima 130 meV, indicates the high crystalline and optical quality of ZnO and very low defect density. Vertically aligned nanosensors were fabricated by depositing gold circular Schottky contacts on ZnO NRs. Resistance responses of nanosensors were observed in the range from 50 to 150 °C in 1% and 5% hydrogen in argon environment, which is below and above the explosive limit (4%) of hydrogen in air. The nanosensor's sensitivity increases from 11% to 67% with temperature from 50 to 150 °C and also shows fast response time (9–16 s) and moderate recovery time (100–200 s). A sensing mechanism is proposed based on Schottky barrier changes at heterojunctions and change in depletion region of NRs. © 2015 AIP Publishing LLC. [<http://dx.doi.org/10.1063/1.4926953>]

I. INTRODUCTION

Gas sensor is one of the emerging applications in nano fabrication since last decade because of its essential requirement in automotive and space application, environment monitoring, domestic sector such as fire alarm and defense organization to detect explosive and hazards gases.^{1–3} Among all other hazards gases, hydrogen is most desirable gas for detection because of its highly flammable nature at high temperature, low flash point and not easy-handling nature.⁴ Hydrogen is widely used in fuel cells, hydrogen engines and biological applications, which provides strong motivations to develop high selectively, compact, and energy efficient hydrogen gas sensor operating at low temperature.^{5,6} ZnO is widely used semiconductor material because of its high electron mobility, intrinsically n type behavior, high chemical and thermal stability under sensor operating conditions.⁷ Gas sensing key parameters like selectivity, sensitivity, response time, recovery time, and stability mainly depend on metal oxide crystallinity, surface to volume ratio, catalyst doping, and operating temperature.^{8,9} 1D nanostructure (nanorods, nanotubes, nanowires, etc.) based gas sensor is most promising technology over thin film based gas sensor technology because of its high surface to volume ratio and miniaturization capability that helps in achieving low temperature gas sensing, enhanced sensitivity and stability.^{10–12} Large surface to volume ratio of nanorods enhances surface adsorption/desorption of hydrogen molecules, which results in massive change in electronic properties and enables lower

limit of detection possible at low operating temperature.¹³ Lupan *et al.*¹⁴ used flexible substrate with focused ion beam approach to fabricate single nanorod based hydrogen sensor. Single nanorod based sensor gives $\sim 4\%$ sensitivity in presence of 200 ppm hydrogen at room temperature (RT). Wang *et al.*¹⁵ studied ZnO nanorods based hydrogen sensor with cluster of Pd, demonstrating enhanced 5 times higher sensitivity than ZnO nanorods for different hydrogen concentration levels at room temperature. Sathanathan *et al.*¹⁶ also reported the effect of Pd doped ZnO 2D nanostructure enhanced sensitivity when compared to undoped ZnO. Operating temperature and hydrogen concentration level also affects gas sensitivity, response time, and recovery time.^{17,18} Park *et al.*¹⁹ fabricated ZnO nanorods (NRs) based chemical sensor on Pt/Si substrate and reported increase in sensitivity when oxygen concentration is increased within the range of 1.4–500 ppm. Al-Salman and Abdullah²⁰ studied the changes of the sensor response for hydrogen concentration varying from 100 ppm to 1000 ppm and temperature varying from RT to 200 °C. These hydrogen sensors shows 24.8% and 99.53% sensitivity when operating temperature is altered from RT to 200 °C. Gas sensor sensitivity and response/recovery time can also be enhanced by Schottky barrier height.²¹ Schottky barrier height can be highly modified by adsorption/desorption of oxygen which in return will radically increase sensor's sensitivity.²² Due to barrier height changes, electron concentration varies at junction which is responsible for the change in resistivity of nano sensors.^{23,24} At low temperature, relative change in resistivity is lesser in comparison to high operating temperature because surface adsorption/desorption reaction of gases enhances with

^{a)}Author to whom correspondence should be addressed. Electronic mail: mkumar@iitj.ac.in.

temperature. Currently, low operating temperature with low level of gas detection using ZnO based nanostructure is prime goal for many researchers. Ranwa *et al.*²⁵ fabricated ZnO NRs/Si Schottky heterojunction based hydrogen sensor which showed fast response time ~ 21.6 s at low operating temperature ($\sim 70^\circ\text{C}$) in pure hydrogen gas. Das *et al.*²⁶ fabricated Pt/ZnO single nanowire Schottky diode by using e-beam lithography. This device gives 90% sensitivity at room temperature with fast response time of about ~ 55 s. Pandis *et al.*²⁷ reported that Au nanocrystal with ZnO improves the sensing response and reduces operating temperature down to 150°C . Wei *et al.*²⁸ also described that the presence of Schottky barrier in addition with ohmic contact enhanced surface chemisorbed reactions and showed 4 times higher sensitivity than ohmic junction. Yu *et al.*²⁹ also reported Pt/nanograined ZnO/SiC Schottky diode based hydrogen nanosensor which gives huge lateral voltage shift (about 173.3 mV and 191.8 mV) in reverse bias for 1% hydrogen and 1% propene at 260°C . In this research work, Au/ZnO NRs based nanosensors are fabricated for hydrogen gas detections.

II. EXPERIMENTAL DETAILS

ZnO nanorods were deposited on *n*-type Si (100) substrate using RF magnetron sputtering system. For eliminating native oxide layer and other contaminations from silicon substrate, chemical cleaning process was performed followed by 5% hydrofluoric acid: 95% deionized water dip. Base pressure was created around 1×10^{-6} mbar and ZnO target was used with $\sim 99.999\%$. Pure argon (99.999% purity) was used as sputtering gas with constant flow of 60 sccm to create plasma. During deposition RF power, chamber pressure and substrate temperature were maintained at 150 W, 2×10^{-2} mbar and 600°C , respectively. Target to substrate distance was fixed around ~ 14 cm and deposition

time was kept 2 h and 15 min. Surface morphology and structural characterizations of the NRs were studied using field emission scanning electron microscopy (FESEM, JSM 7100F, Jeol) and X-ray diffraction (XRD, Bruker D8 Advance). Near-band and visible-range emission spectra were acquired using cathodoluminescence (CL) spectroscopy apparatus (MONO CL4, Gatan) coupled with the FESEM, and operated with 7 nm bandwidth (~ 0.06 eV at 3.24 eV). Circular dots of $500 \mu\text{m}$ diameter and 200 nm thick Au Schottky contacts were deposited by thermal evaporation with the help of physical mask. Spacing between two circular dots is around $\sim 500 \mu\text{m}$. Nanosensor devices were characterized in vacuum chamber with 2×10^{-3} mbar base chamber pressure and external heater was used to vary the temperature from RT to 150°C . The measurements were performed with 1% and 5% hydrogen in argon concentrations, which is below and above the explosive limit (4%) of hydrogen in air. The chamber pressure changes approximately 5 mbar while loading/deloading hydrogen in vacuum chamber. Resistivity with respect to time was measured at operating temperature (50 – 150°C) with two hydrogen concentrations (1% and 5%) using Keithley semiconductor characterization system (4200).

III. RESULTS AND DISCUSSION

Surface morphologies of ZnO NRs were investigated by FESEM and AFM. Figs. 1(a)–1(c) show top view, tilted view, and cross sectional view of NRs, and from the FESEM images, it can be observed that the NRs are well-aligned and uniformly distributed throughout the Si substrate. Height, average diameter, and distribution density of NRs were determined to be ~ 850 nm, ~ 76 nm, and $\sim 1.5 \times 10^{10} \text{cm}^{-2}$, respectively. Average size, density, and distribution of ZnO NRs are also verified by AFM and shown in Fig. 1(d). Fig. 2(a) shows 2θ - ω

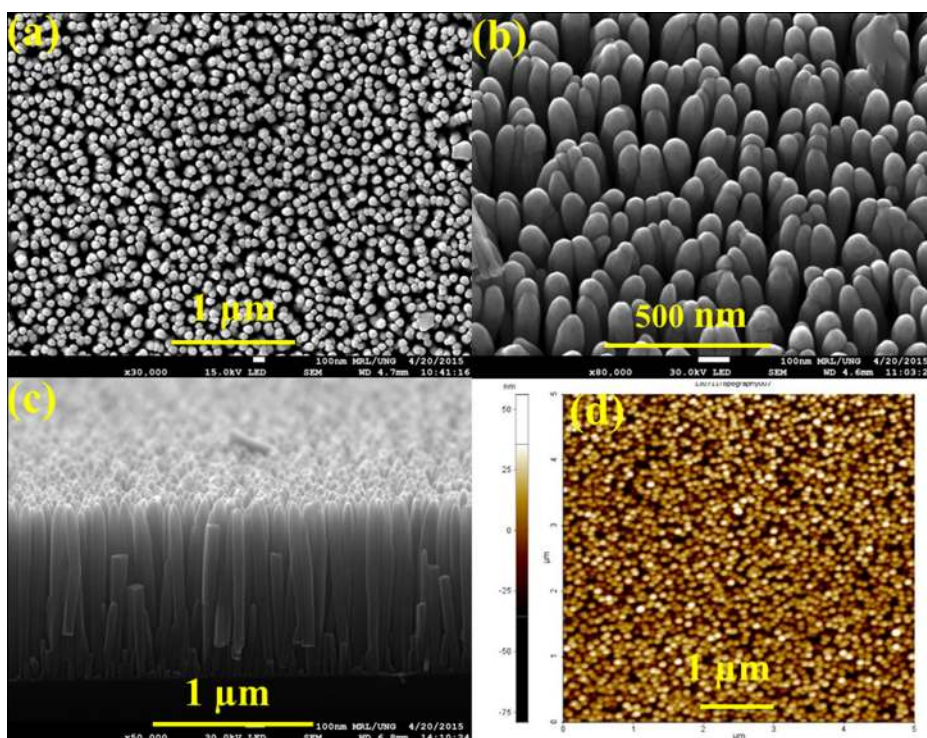


FIG. 1. (a)–(c) Top view, tilted view (17° off normal), and cross sectional view (87° off normal) of FESEM images and (d) AFM 2D image.

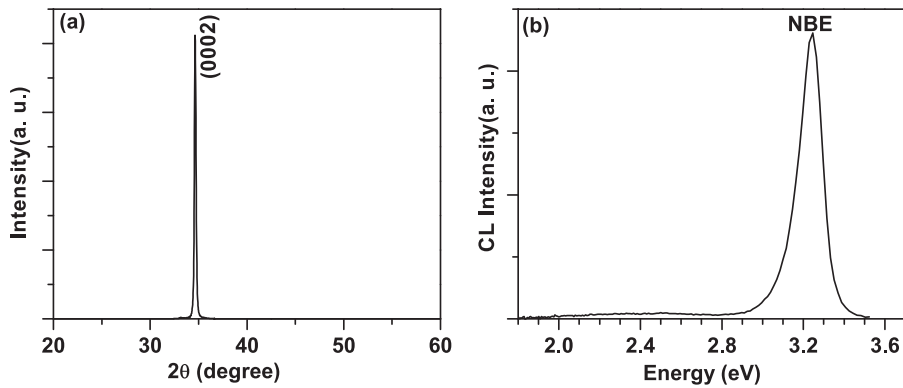


FIG. 2. (a) 2θ - ω scan of X-ray diffraction pattern and (b) CL spectra of NRs.

scan of XRD which shows only one strong peak at 34.64° corresponding to wurtzite ZnO with full width half maxima (FWHM) $\sim 0.21^\circ$. XRD and FESEM clearly show that ZnO NRs are grown along (0002) direction.³⁰ In CL spectra, shown in Fig. 2(b), a strong peak is observed at 3.24 eV with FWHM ~ 0.13 eV corresponding to near band-edge emission (NBE) peak, which is attributed to recombination of free exciton.³¹ The presence of a strong and sharp NBE peak and the almost complete absence of broad peak in visible range indicate high optical properties of ZnO NRs and absence or very low density of traps/defects centres.³²

Hydrogen gas sensing properties of nanosensor were measured at two Au Schottky contacts as shown as schematic diagram in Fig. 3(a). The nanosensor has four Schottky contacts, two between Au and ZnO NRs and two between NRs and Si substrate. Schottky barrier height between Au/ZnO NRs and ZnO NRs/n-Si can be determined using electron affinity model (EAM). The Schottky barrier height at Au/ZnO is $\phi_B = \phi_M - \chi_{\text{ZnO}}$ and conduction band and valance band offsets at ZnO/Si are $\Delta E_C = \chi_{\text{ZnO}} - \chi_{\text{Si}}$ and $\Delta E_V = E_{g,\text{ZnO}} - E_{g,\text{Si}} + \Delta E_C$. For Au $\phi_M = 5.1$ eV, $\chi_{\text{ZnO}} = 4.35$, $\chi_{\text{Si}} = 4.05$, $E_{g,\text{ZnO}} = 3.24$ eV, and $E_{g,\text{Si}} = 1.12$ eV.³³ The resulting value for Schottky barrier height is $\phi_B \sim 0.78$ eV and conduction band offset is $\Delta E_C \sim 0.3$ eV.

Fig. 3(b) depicts I-V characteristics of Au/ZnO NRs/Si/ZnO NRs/Au Schottky junction at 75°C without hydrogen and with 1% and 5% hydrogen concentration. I-V plot shows rectifying behavior due to the presence of Schottky junction at ZnO/Si as well as Au/ZnO heterojunction. With exposure

of 1% and 5% hydrogen concentration in argon, Schottky barrier height decreases which enhances current as well as lateral voltage shift observe in comparison to air. Figs. 3(c) and 3(d) show the resistivity response curve with time of Au/ZnO NRs/Si/ZnO NRs/Au heterojunction based nanosensor device at 100°C operating temperature for 1% hydrogen and 5% hydrogen in pure Argon concentration, respectively. The flammability limit of hydrogen is around 4% in air and the testing concentration was chosen below and above this limit. The curve clearly shows that resistance changes can be affected by hydrogen concentration at particular operating temperature. It can also be observed that change in resistance is dominating up to certain level of hydrogen concentration, beyond which it increases slowly and becomes saturated for constant operating temperature. Temperature dependent resistive response of the nanosensor in 1% and 5% hydrogen in pure argon concentration is shown in Figs. 4(a) and 4(b). As operating temperature increases from 50°C to 150°C , rate of adsorption/desorption reaction of reactive gases increases with temperature. From the figure, it can be seen that the base resistance decreases with increasing operating temperature. This is due to the following two reasons: (i) the resistance decreases with increasing temperature in the semiconductors and (ii) Schottky barrier height also decreases with temperature which also reduces the resistance. It can also be observed that the changes in resistance are relatively smaller for 5% in comparison to 1% hydrogen at particular operating temperature due to the saturation of response. Schottky metal junctions such as Pt, Pd, and Au can enhance the gas sensitivity of ZnO NR based gas sensors.^{22-24,34} In

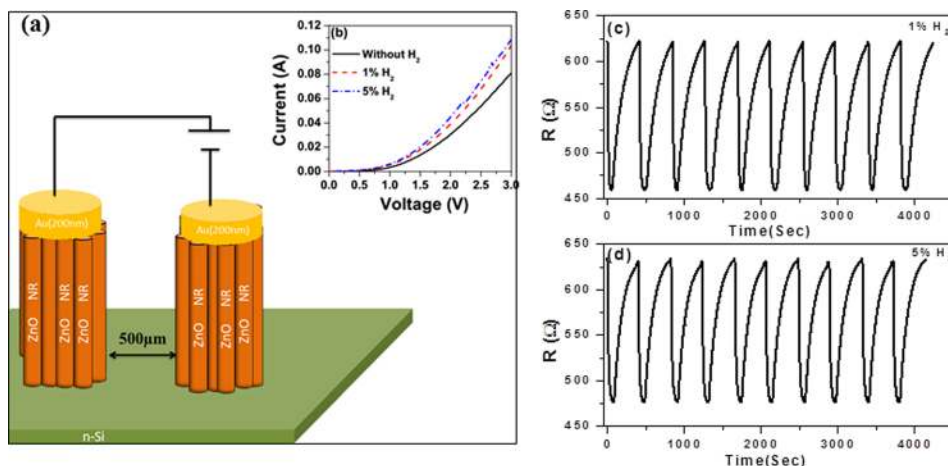


FIG. 3. (a) Schematic diagram of nanosensor. (b) I-V characteristics of nanosensor at 75°C without hydrogen and with 1% and 5% hydrogen concentration. (c) and (d) Resistance response curve with time at 100°C for 1% and 5% hydrogen concentration, respectively.

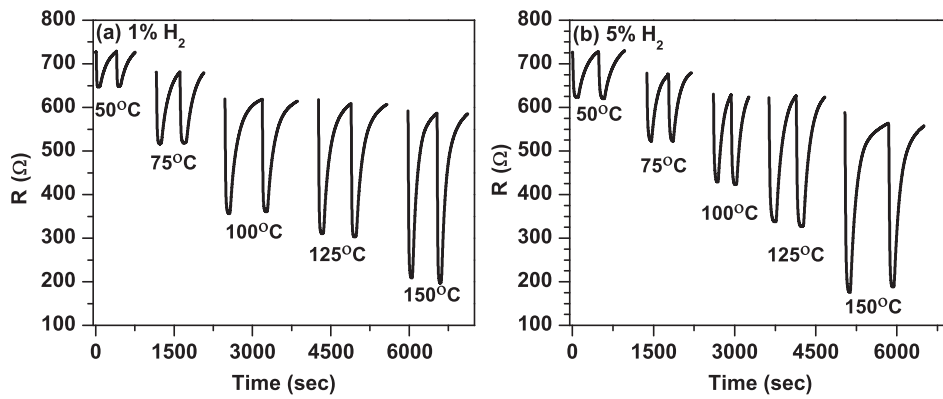


FIG. 4. Temperature dependent resistive response curve for (a) 1% hydrogen and (b) 5% hydrogen in argon.

the present work, ZnO NR as well as Au/ZnO NRs and ZnO NRs/Si Schottky junctions plays an important role in hydrogen sensing. Adsorption/desorption of reactive gases takes place at ZnO NRs as well as at Schottky junction. Upon exposition to of hydrogen gas, adsorption/desorption process takes places at Au/ZnO Schottky junction and Au acts as a catalyst for hydrogen adsorption similar to Pt and Pd metals.²⁷ In gas sensing, hydrogen molecule diffused in Au electrodes, which causes variation of barrier height at Au/ZnO junctions and increases the sensitivity.

Gas sensor performance is based on its characteristics like response time, recovery times and sensitivity. Exponential increase in resistance allows evaluation of recovery or rise time (τ_r), and exponential decrease in resistance allows evaluation of response or decay time (τ_d), as given by the equations,³⁵

$$R = R_0 + A \exp\left(\frac{t}{\tau_r}\right), \quad (1)$$

$$R = R_1 + B \exp\left(-\frac{t}{\tau_d}\right), \quad (2)$$

where A and B are scaling constants. The rise and decay times are extracted from experimental data by fitting with Eqs. (1) and (2), as shown in Figs. 5(a) and 5(b) for 1% and 5% hydrogen concentration at 100 °C operating temperature. Figs. 6(a) and 6(b) show response time and recovery time vs temperature for 1% and 5% hydrogen concentration. Response time increases from 9.4 s to 12 s for 1% hydrogen with temperature for low temperature range (up to 100 °C) and then almost remains constant in temperature range from 100 to 150 °C. For 5% hydrogen, due to relatively higher concentration, response time decreases with increasing temperature (up to 100 °C) from 16 to 12 s then for higher operating temperature becomes almost constant. Recovery time is highly influenced by operating temperature. Recovery time varies from approximately 200 s to 120 s for 1% hydrogen concentration as operating temperature varies in the range of 50–150 °C. At higher hydrogen concentration (5%) the dependence on temperature variation is more pronounced. For increasing working temperature, more oxygen ions are adsorbed at ZnO NRs which creates depletion region. During hydrogen loading process, these hydrogen molecules react with oxygen

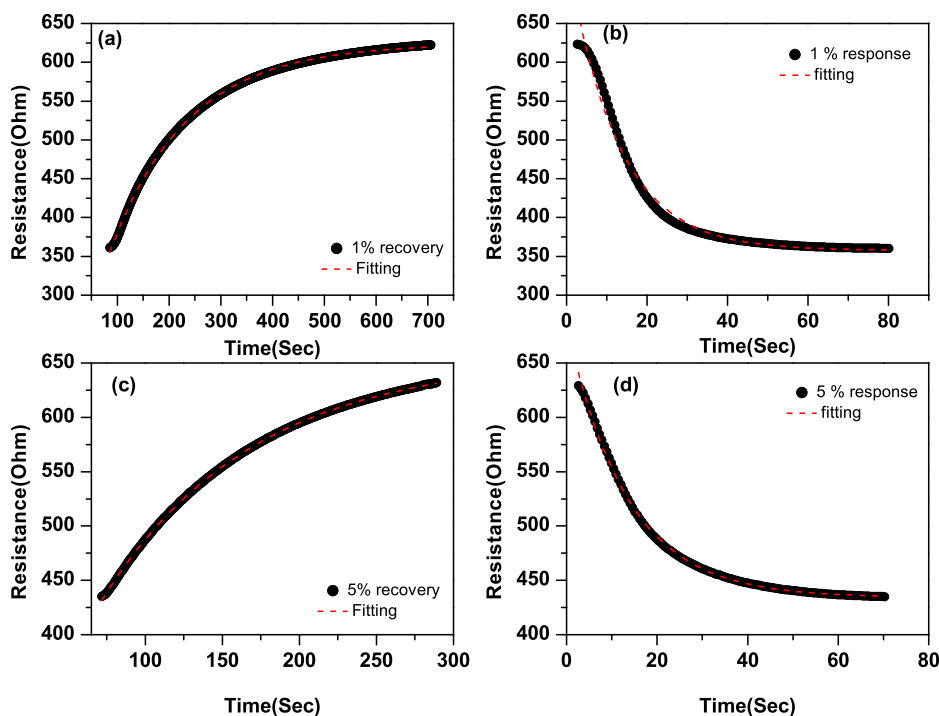


FIG. 5. (a)–(d) The rise and decay time exponential fitting of 1% hydrogen and 5% hydrogen concentration resistive response curve at 100 °C, respectively.

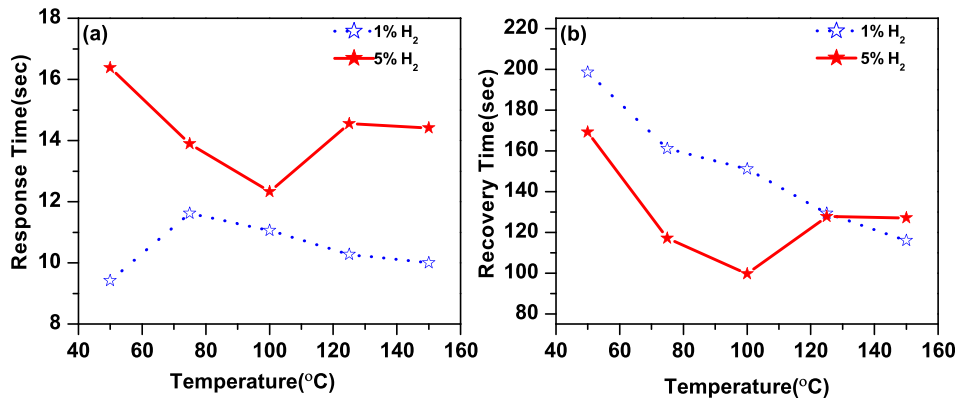


FIG. 6. (a) and (b) Response time, recovery time in the presence of 1% and 5% hydrogen with temperature range varies from 50 °C to 150 °C.

species and decrease depletion region. The resulting fast recovery is due to large number of available free electrons. At operating temperature 100 °C, nanosensor shows recovery time around ~ 150 s for 1% hydrogen and around ~ 100 s 5% hydrogen concentration. Large change in recovery time with hydrogen concentration depicts more ions of hydrogen react with oxygen ions and decreases depletion region.

Gas sensitivity is defined as relative change in resistance with respect to resistance in presence of air. It is given as³⁶

$$S = \left(\frac{R_a - R_g}{R_a} \right) \times 100\%.$$

Fig. 7 shows sensitivity vs temperature curve at different hydrogen concentrations, which clearly indicates that sensitivity increases linearly with operating temperature. Sensitivity increases from 11% to $67 \pm 2\%$ with increasing operating temperature from 50 °C to 150 °C. The variation in sensitivity behavior is very low between 1% and 5% hydrogen concentration because of saturation of NRs as well as Schottky contact. Beyond 1% hydrogen concentration, sensitivity increases with temperature but not drastically. Relative change in resistance is $41 \pm 2\%$ and $34 \pm 2\%$ for 1% and 5% hydrogen concentration at 100 °C,

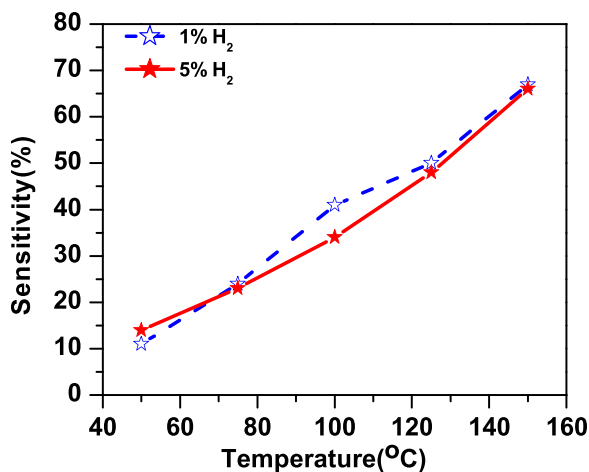


FIG. 7. Sensitivity versus temperature curve for varying hydrogen concentration.

respectively. The above results suggest that nanosensor shows fast response time (9–12 s) and moderate sensitivity ($11\text{--}67 \pm 2\%$) at operating temperature below 150 °C. Au/ZnO nanorods based Schottky junction based nanosensor is showing fast response time as compared to recently reported undoped/doped ZnO nanostructures at low operating temperature.^{37,38} Hassan *et al.*³⁷ reported that Pt/ZnO nanorods based sensor shows 200 s response time with high sensitivity at 100 °C. Alam *et al.*³⁸ also reported Pd nanocubes decorated ZnO nanorods based hydrogen sensor which gives high response time 1.98 min at 100 °C for 1% hydrogen concentration.

Figs. 8(a) and 8(b) show the schematic diagram of proposed gas sensing mechanism and Figs. 8(c) and 8(d) depict energy level diagram of Au/ZnO NRs interface in the presence of hydrogen at forward and reverse bias, respectively. When ZnO NRs come in contact with atmospheric oxygen and gases, oxygen molecules adsorb on ZnO NRs surface and extract electron from conduction band. This creates adsorbed oxygen (O^- , O_2^- , O^{2-}) ions on nanorods surface and creates depletion region in nanorods.³⁶ Adsorption of oxygen decreases electron concentration in ZnO NRs and resistance of device increases. When ZnO nanorods are exposed to hydrogen, H₂ molecules react with adsorbed oxygen, electron concentration in conduction band increases, and resistance of ZnO nanorods decreases. These chemisorbed reactions are highly temperature dependent and also influenced by hydrogen concentration. For low temperature and for low hydrogen concentration, Schottky junctions play an important role, and due to the adsorption of hydrogen molecules at Schottky junction, barrier height changes.³⁹ When hydrogen molecules react with Au contact, they dissociated into hydrogen atoms.²⁷ Dissociated hydrogen atoms form dipole layer at Au/ZnO NR interface layer and create electric field at junction. Effective barrier height as well as metal work function reduces because of hydrogen atom diffusion. In forward bias at Au/ZnO NRs junction, electrons use dipoles as tunneling junctions, and it increases current as well as reduces resistance at junction. In reverse bias—also due to presence of these dipoles—low reverse bias voltage is required to cross the barrier height by tunneling. This barrier height variations support an increased conductivity of Au/ZnO NR heterojunction in comparison to ohmic contact. In summary, gas sensitivity and recovery time are highly

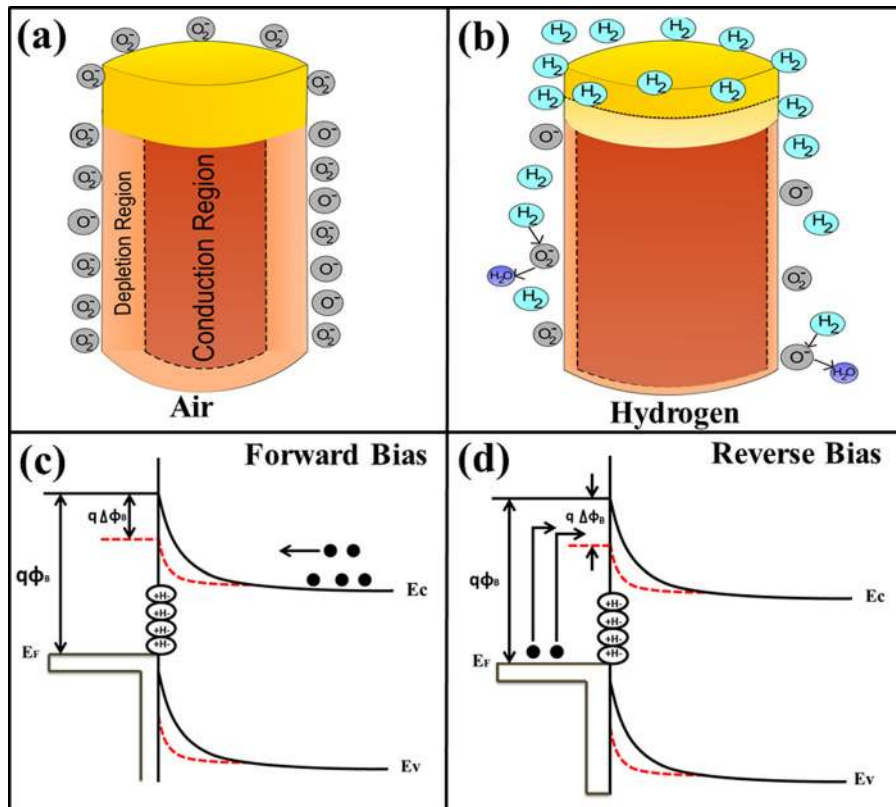


FIG. 8. (a) and (b) Schematic diagram of proposed gas sensing mechanism and (c) and (d) forward and reverse bias at Schottky junction.

influenced by what is occurring both at ZnO NRs surface and at Schottky junctions, since the nanosensor performances are highly influenced by hydrogen loading/deloading induced variation of depletion width in ZnO NRs and of Schottky barrier height.

IV. CONCLUSION

Vertically aligned ZnO NRs with high aspect ratio were deposited on n-Si using RF sputtering technique. Wurtzite crystalline structure of ZnO NRs was confirmed by XRD. FESEM images show uniform distribution of ZnO NRs on entire silicon substrate. CL spectra show strong NBE emission at approximately 3.24 eV without emission in the green-yellow region, indicating good optical and crystalline properties with low defect density. Au/ZnO NRs/Si/ZnO NRs/Au Schottky junction based nanosensor was fabricated and tested at different temperatures with 1% and 5% hydrogen environment. Proposed device gives fast response ~ 14 s for 1% hydrogen and 12.8 s for 5% hydrogen at operating temperature 100 °C. The recovery times were determined ~ 100 and 150 s for 1% and 5% hydrogen concentrations, respectively. Sensitivity of gas sensor is highly dependent on temperature and varies from ~ 11 to $67 \pm 2\%$ for both hydrogen concentrations, as operating temperature increases from 50 °C to 150 °C. For best response and recovery time, sensitivity is approximately 34%–41% for both hydrogen concentrations at operating temperature 100 °C. The presence of Schottky metal contact and the high aspect ratio of ZnO NRs both play an important role in achieving an enhanced sensor response at low

operating temperature and in the low hydrogen concentration regime (up to 5%).

ACKNOWLEDGMENTS

The authors acknowledge the financial support from Department of Atomic Energy (DAE) Project No. 34/14/16/2014-BRNS with ATC.

- ¹B. Timmer, W. Olthuis, and A. V. D. Berg, *Sens. Actuators, B* **107**, 666 (2005).
- ²X. Liu, S. Cheng, H. Liu, S. Hu, D. Zhang, and H. Ning, *Sensors* **12**, 9635 (2012).
- ³M. M. Arafat, B. Dinan, S. A. Akbar, and A. S. M. A. Haseeb, *Sensors* **12**, 7207 (2012).
- ⁴M. T. Soo, K. Y. Cheong, and A. F. M. Noor, *Sens. Actuators, B* **151**, 39 (2010).
- ⁵O. Lupan, L. Chow, T. Pauporté, L. K. Ono, B. R. Cuenya, and G. Chai, *Sens. Actuators, B* **173**, 772 (2012).
- ⁶P. Zhang, A. Vincent, A. Kumar, S. Seal, and H. J. Cho, *IEEE Electron Device Lett.* **31**(7), 770 (2010).
- ⁷U. Ozgur, Ya. I. Alivov, C. Liu, A. Teke, M. A. Reshchikov, S. Dogan, V. Avrutin, S.-J. Cho, and H. Morkoç, *J. Appl. Phys.* **98**, 041301 (2005).
- ⁸H. Gu, Z. Wang, and Y. Hu, *Sensors* **12**, 5517 (2012).
- ⁹V. E. Bochenkov and G. B. Sergeev, *Metal Oxide Nanostructures and Their Applications* (American Scientific Publishers, 2010), Vol. 3, pp. 31–52.
- ¹⁰S. Deshpande, A. Karakoti, G. Londe, H. J. Cho, and S. Seal, *J. Nanosci. Nanotechnol.* **7**, 3354 (2007).
- ¹¹K. J. Choi and H. W. Jang, *Sensors* **10**, 4083 (2010).
- ¹²J. G. Lu, P. Chang, and Z. Fan, *Mater. Sci. Eng.* **R 52**, 49 (2006).
- ¹³T. Anderson, F. Ren, S. Pearton, B. S. Kang, H.-T. Wang, C. Y. Chang, and J. Lin, *Sensors* **9**, 4669 (2009).
- ¹⁴O. Lupan, G. Chai, and L. Chow, *Micro Eng.* **85**, 2220 (2008).
- ¹⁵H. T. Wang, B. S. Kang, F. Ren, L. C. Tien, P. W. Sadik, D. P. Norton, S. J. Pearton, and J. Lin, *Appl. Phys. Lett.* **86**, 243503 (2005).
- ¹⁶S. Sathananthan, V. P. Dravid, and S. W. Fan, *Nanoscape* **6**, 6 (2009).
- ¹⁷L. J. Bie, X. Yan, J. Yin, Y. Q. Duan, and Z. H. Yuan, *Sens. Actuators, B* **126**, 604 (2007).

- ¹⁸N. L. Hung, E. Ahn, S. Park, H. Jung, H. Kim, S. K. Hong, and D. Kim, *J. Vac. Sci. Technol., A* **27**, 1347 (2009).
- ¹⁹J. Y. Park, S. W. Choi, and S. S. Kim, *Nanoscale Res. Lett.* **5**, 353 (2010).
- ²⁰H. S. Al-Salman and M. J. Abdullah, *Sens. Actuators, B* **181**, 259 (2013).
- ²¹J. Zhou, Y. Gu, Y. Hu, W. Mai, P. H. Yeh, G. Bao, A. K. Sood, D. L. Polla, and Z. L. Wang, *Appl. Phys. Lett.* **94**, 191103 (2009).
- ²²Q. G. Al-Zaidi, A. M. Suhail, and W. R. Al-Azawi, *Appl. Phys. Res.* **3**, 89 (2011).
- ²³J. Yu, S. J. Ippolito, W. Wlodarski, M. Strano, and K. Kalantar-zadeh, *Nanotechnology* **21**, 265502 (2010).
- ²⁴M. Shafiei, J. Yu, R. Arsat, K. Kalantar-Zadeh, E. Comini, M. Ferroni, G. Sberveglieri, and W. Wlodarski, *Sens. Actuators, B* **146**, 507 (2010).
- ²⁵S. Ranwa, P. K. Kulriya, V. K. Sahu, L. M. Kukreja, and M. Kumar, *Appl. Phys. Lett.* **105**, 213103 (2014).
- ²⁶S. N. Das, J. P. Kar, J. H. Choi, T. Lee, K. J. Moon, and J. M. Myoung, *J. Phys. Chem. C* **114**, 1689 (2010).
- ²⁷C. Pandis, N. Brilis, E. Bourithis, D. Tsamakis, H. Ali, S. Krishnamoorthy, A. A. Iliadis, and M. Kompitsas, *IEEE Sens. J.* **7**, 448 (2007).
- ²⁸T. Y. Wei, P. H. Yeh, S. Y. Lu, and Z. L. Wang, *J. Am. Chem. Soc.* **131**, 17690 (2009).
- ²⁹J. Yu, M. Shafiei, C. M. Oh, T. B. Jung, K. Kalantar-Zadeh, J. H. Kang, and W. Wlodarski, *Sens. Lett.* **9**, 55 (2011).
- ³⁰Y. Sun, G. M. Fuge, and M. N. R. Ashfold, *Chem. Phys. Lett.* **396**, 21 (2004).
- ³¹D. V. Myroniuk, G. V. Lashkarev, I. I. Shteplyuk, V. A. Skuratov, A. Reszka, and B. J. Kowalski, *Acta Phys. Pol., A* **126**, 1199 (2014).
- ³²C. Chandrinou, N. Boukos, C. Stogiou, and A. Travlos, *Microelectron. J.* **40**, 296 (2009).
- ³³S. Ranwa, P. K. Kulriya, V. Dixit, and M. Kumar, *J. Appl. Phys.* **115**, 233706 (2014).
- ³⁴C. S. Rout, G. U. Kulkarni, and C. N. R. Rao, *J. Phys. D: Appl. Phys.* **40**, 2777 (2007).
- ³⁵A. Z. Adamyan, Z. N. Adamyan, V. M. Aroutiounian, K. D. Schierbaum, and S. D. Han, *Arm. J. Phys.* **2**, 200 (2009).
- ³⁶O. Lupan, V. V. Ursaki, G. Chai, L. Chow, G. A. Emelchenko, I. M. Tiginyanu, A. N. Gruzintsev, and A. N. Redkin, *Sens. Actuators, B* **144**, 56 (2010).
- ³⁷J. J. Hassan, M. A. Mahdi, C. W. Chin, H. Abu-Hassan, and Z. Hassan, *Sens. Actuators, B* **176**, 360 (2013).
- ³⁸M. F. B. Alam, D. T. Phan, and G. S. Chung, *Mater. Lett.* **156**, 113 (2015).
- ³⁹J. Yu, M. Shafiei, M. Breedon, K. Kalantar-Zadeh, and W. Wlodarski, *Procedia Chem.* **1**, 979 (2009).